

HOCO⁺ toward the Galactic Center

Shuji DEGUCHI,¹ Atsushi MIYAZAKI,^{1,2}

and

Young Chol MINH^{3,4}

¹ *Nobeyama Radio Observatory, National Astronomical Observatory,
Minamimaki, Minamisaku, Nagano 384-1305*

² *Shanghai Astronomical Observatory, Chinese Academy of Sciences
80 Nandan Road, Shanghai, 200030, P.R. China*

³ *Korea Astronomy and Space Science Institute,
61-1 Hwaam, Yuseong-ku, Daejeon 305-348, Korea*

⁴ *Academy Sinica, Institute of Astronomy and Astrophysics, P.O. Box 23-141, Taipei 106, Taiwan*

(Received 2006 July 10; accepted ; Ver 1.1 Sept 18, 2006)

Abstract

We have identified a weak thermal line U42.767, which has been detected only in the directions toward Sgr A and Sgr B2, as the HOCO⁺ $2_{02}-1_{01}$ transition. Because of the proximity of this line to the SiO maser line at 42.821 GHz ($J = 1-0$ $v = 2$), it was observable simultaneously in the ~ 43 GHz SiO maser searches at Nobeyama. From the past data of SiO maser surveys of infrared objects in the Galactic center, we created a map of emission distribution of HOCO⁺ in the Sgr A molecular cloud as well as maps of the ^{29}SiO $J = 1-0$ $v = 0$ thermal emission and H53 α emission. The emission distribution of HOCO⁺ was quite similar to the distribution of ^{29}SiO emission. It suggests that the enhancement of the HOCO⁺ abundance in the galactic center is induced by shock activities which release the CO₂ molecules frozen on grains into gases.

Key words: Galaxy: center — ISM: molecules — line: identification — molecular data

1. Introduction

In the course of the past SiO maser line observations in the 43 GHz band at Nobeyama, we noticed that several weak unidentified lines occasionally contaminated the spectra toward stars in the Galactic center (Deguchi et al. 2002; Deguchi et al. 2004). They are not listed

in the catalog of known molecular lines compiled by Lovas et al. (2004).¹ Among these, the unidentified line, U42.767, bothered us strongly because it appears near the SiO $J = 1-0$ $v = 2$ line at 42.821 GHz with a velocity separation of about 380 km s⁻¹, making a false signal of extreme high-velocity maser emission toward the Galactic center. The width of this unidentified line was quite broad compared with SiO maser lines, indicating that it is thermal emission from molecular clouds. On the high frequency side of the SiO line, the other weak lines of ²⁹SiO $J = 1-0$ $v = 0$ line ($\Delta V = -416$ km s⁻¹) and H53 α ($\Delta V = -921$ km s⁻¹) also contaminate the SiO maser spectra. A comparison of emission intensities between U42.767, ²⁹SiO, and H53 α suggested that U42.767 appears only in a relatively dense region of molecular clouds in the Galactic center. So far, we have surveyed toward many AGB stars in the Galactic bulge and disk, and several molecular clouds such as Ori A, TMC1, and W51 in these lines, but we did not detect U42.767 except in the Galactic center region (see Izumiura et al. 1995; Miyazaki et al. 2001; Kaifu et al. 2004).

By checking the JPL catalog of Molecular Spectroscopy (Pickett et al. 1998),² we found that one of the best candidates for U42.767 is the HOCO⁺ $2_{02}-1_{01}$ transition (42766.2 MHz). The other rotational lines of this molecule have been detected only in the molecular clouds toward the Galactic center: Sgr A and Sgr B2 (Thaddeus et al. 1981; Minh et al. 1988).

In 2001–2003, we made a large SiO maser survey of about 400 stars within 15' of Sgr A* (Imai et al. 2002; Deguchi et al. 2004). This survey took the data of the above three lines in one spectrometer with a band width of 250 MHz, together with the SiO $J = 1-0$ $v = 2$ maser line. In this paper, we describe the result of mapping in these three lines toward the Sgr A molecular cloud. The emission distribution of U42.767 was quite similar to the distribution of the HOCO⁺ $4_{04}-3_{03}$ line at 85.531 GHz obtained before by Minh et al. (1991). Based on all of these results, we conclude that U42.767 is the HOCO⁺ $2_{02}-1_{01}$ transition.

2. Observational data and results

We used the spectral data taken by an acousto-optical spectrometer with 250 MHz band width (AOS-W) in the course of an SiO maser survey of the large amplitude variables in the Galactic center (Imai et al. 2002). In these observations, data at the positions of about 400 stars toward the Galactic center (within 15' from Sgr A*) were obtained during 2001–2003 with the 45-m radio telescope at Nobeyama. The effective frequency resolution of the AOS-W spectrometer is 250 kHz (1.75 km s⁻¹). The overall system temperature was between 200 and 300 K, depending on weather condition. The half-power telescope beam width (HPBW) was about 40'' and the beam efficiency at 43 GHz was 0.77. Typical rms noise level in the spectra was about 0.03 K. Further details of SiO maser observations using the NRO 45-m telescope

¹ For latest compilation available in <http://physics.nist.gov/PhysRefData/Micro/Html/contents.html>.

² The latest version is available at <http://spec.jpl.nasa.gov/>

have been described elsewhere (Deguchi et al. 2004), and are not repeated here. The AOS-W spectra occasionally exhibited considerable baseline distortions. We applied a parabolic baseline removal to the individual spectra and extracted intensities of the $\text{HOCO}^+ 2_{02}-1_{01}$, $^{29}\text{SiO } J=1-0 \ v=0$, and $\text{H53}\alpha$ transitions from the spectra. The rest frequencies used are given in table 1. Because the lines were weak and because standing-wave features (appearing occasionally) could not be removed completely, we discarded a few bad data. The data points used in the map making are not uniformly distributed for the three mapped lines: the number of points used for map making are 369, 370, and 347 for the $\text{HOCO}^+ 2_{02}-1_{01}$, $^{29}\text{SiO } J=1-0$, and $\text{H53}\alpha$ lines. Because of non-uniform sampling of the observed points, we applied a $140''$ Gaussian smoothing in the map making; the effective spatial resolution in the created map was lowered in this procedure.

Figure 1 shows the AOS-W spectra toward the SiO maser sources [GMC2001] 12–13 (=V5038 Sgr; see Glass et al. 2001 or Deguchi et al. 2004) and Sgr B2 MD5; the latter does not exhibit the SiO $J=1-0 \ v=2$ emission (see Shiki et al. 1997). Adjacent to the SiO $J=1-0 \ v=2$ maser line at 42.821 GHz, the $\text{HOCO}^+ 2_{02}-1_{01}$, $^{29}\text{SiO } J=1-0$, and $\text{H53}\alpha$ lines are recognizable. Figures 2a–2c show the integrated intensity maps of the above three lines toward the Galactic center. The velocity channel maps (combined in every 20 km s^{-1}) are also shown in figures 3a–3c. Figure 2a indicates that the emission distribution is quite similar to the $\text{HOCO}^+ 4_{04}-3_{03}$ emission shown in figure 1b of Minh et al. 1991, suggesting the validity of identification of U42.767 to this molecule; both transitions have triple intensity peaks at $(l, b) = (0.11^\circ, -0.08^\circ)$, $(0.01^\circ, -0.07^\circ)$ and $(-0.13^\circ, -0.08^\circ)$.

We also checked the more recent AOS-W data taken by the 2004–2005 SiO maser survey toward the $7^\circ \times 2^\circ$ area of the Galactic center (Fujii et al. 2006). The surveyed area covered the Sgr C molecular cloud (G395.43–00.09). However, no HOCO^+ emission stronger than 0.10 K was detected, especially toward MSX objects near Sgr C: G359.2871–00.2009, G359.3258+00.0040, G359.3819+00.0049, and G359.5035–00.1073. The Sgr C cloud, as well as Sgr A and B clouds, is known as a 6.4 keV X-ray reflection cloud (Murakami et al. 2003).

3. Discussion

3.1. Chemistry and excitation of HOCO^+

The HOCO^+ molecule (protonated carbon dioxide) is thought to form via a standard ion-molecule reaction, the transfer of a proton from H_3^+ to CO_2 (Herbst et al. 1977; Turner et al. 1999). Interestingly, the extensive survey of the HOCO^+ toward various Galactic objects revealed that this molecule is exclusively abundant only toward our Galactic center region (Minh et al. 1988; 1991). Since HOCO^+ is the protonated ion of CO_2 , the enhancement of the HOCO^+ abundance may suggest an increase of the gas phase CO_2 abundance. Though CO_2 may be an important reservoir of interstellar carbon and oxygen, the lack of an electric dipole

moment of this symmetric molecule made gas phase detections difficult. Observations of the 15 μm band of CO_2 from space indicate that the observed gas-phase CO_2 abundances are typically $\sim 2 \times 10^{-7}$ toward various star-forming regions, which is up to two orders of magnitude lower than those of solid CO_2 in the same regions (van Dishoeck 2004).

The chemistry connecting CO_2 with HOCO^+ is not completely clear. However, if HOCO^+ forms by the reaction with the gas phase CO_2 , the large enhancement of HOCO^+ in our Galactic center indicates that the special environment of the Galactic center is necessary to enhance the CO_2 abundance exclusively in this region.

Excitation of the HOCO^+ rotational levels was discussed extensively in Minh et al. (1991). The observed line intensity ratio of $4_{04}-3_{03}$ to $2_{02}-1_{01}$ is 1.56 at the HOCO^+ peak position $[(l, b) = (0.11^\circ, -0.08^\circ)]$, which gives a rotational temperature of 7.0 K (assuming the lines to be optically thin), and the HOCO^+ column density of $\sim 4.2 \times 10^{13} \text{ cm}^{-2}$. [At this position the excitation of HOCO^+ may not be affected much by the background infrared radiation field which can enhance the b -type transitions of this slightly asymmetric top, as was discussed by Minh et al. (1991) in their excitation model calculation.] In order to derive the fractional abundance of HOCO^+ , we use the total H_2 column density, $\sim 6 \times 10^{22} \text{ cm}^{-2}$, derived by Minh et al. (2005) at this position. Then, we obtain the fractional abundance of HOCO^+ , $\sim 7 \times 10^{-10}$, relative to H_2 ; this value is about an order of magnitude less than the one derived using an excitation model previously by Minh et al. (1991). The fractional abundance of $\sim 10^{-9}$ is still much larger, by more than an order of magnitude, than the value expected from the gas phase reactions (see discussions in Minh et al. 1988). However, if we apply the large H_2 column density, $\sim 6 \times 10^{23} \text{ cm}^{-2}$, suggested by Handa et al. (2006) at G 0.11–0.11, the fractional abundance of HOCO^+ will be lowered as well. The abundances for this cloud, which shows an HCO^+ enhancement (Minh et al. 2005), will be further discussed in the following section. We think that the HOCO^+ peaks in the Sgr A region certainly trace a specific physical condition which can increase the HOCO^+ formation, such as the shock induced grain evaporation. HOCO^+ also shows, unlike most other molecules, a unique distribution in Sgr B2, which strongly suggests that the formation of this molecule needs a specific condition existing exclusively in our Galactic center (Minh et al. 1998).

3.2. the Galactic center molecular clouds

The region within $\sim 20'$ from the Galactic center (Sgr A*) is one of the best investigated areas in various molecular/atomic lines and continuum (for example, see Oka et al. 1998; Tuboi et al. 1999). There are several dense molecular clouds including Sgr A East (Güsten et al. 1981; Armstrong et al. 1985) and G0.11–0.11 (Handa et al. 2006); the latter is known to have an extremely high H_2 column density (Handa et al. 2006). However, the molecular clouds in this area are known to be clumpy; Miyazaki & Tsuboi (2000) analyzed the mass spectra of the clumps using CS emission in this area.

Though the general morphology of HOCO^+ emission in figure 2a is similar to the previous results obtained from the $4_{04} - 3_{03}$ transition (figure 1b of Minh et al. 1991), it shows slightly higher contrast, partially due to different position sampling and applied smoothing ("random" sampling in this paper), and partially due to the excitation of the two observed transitions (the excitation energies from the ground state to the 2_{02} and 4_{04} levels are about 3 and 10 K, respectively). The rightmost bright clump corresponds to the gas condensation M-0.13 - 0.08 (indicated by the rightmost filled square in figure 2a), which is known as the +20 km s $^{-1}$ cloud. Minh et al. (2005) argued that the cloud M-0.13 - 0.08 consists of two different velocity components, the 5 km s $^{-1}$ and 25 km s $^{-1}$ components, based on the chemical differences and steep velocity gradient. The 25 km s $^{-1}$ cloud is located near to the expanding SNR Sgr A East and is thought to be interacting with it directly (Okumura et al. 1991; Ho et al. 1991; Coil et al. 2000). The HOCO^+ $4_{04} - 3_{03}$ emission peaks toward the center of the +25 km s $^{-1}$ cloud, but the $2_{02} - 1_{01}$ emission peaks at the position $2'-3'$ lower in b . However, this is probably an artifact due to undersampling of the observed positions at the lower part of this cloud. The line intensity ratio of the $2_{02} - 1_{01}$ to $4_{04} - 3_{03}$ transition suggests a considerably high excitation temperature ($\gtrsim 200$ K) at the center of M-0.13 - 0.08. If the +25 km s $^{-1}$ component is interacting with Sgr A East toward the Galactic center, the high excitation temperature may indicate that the HOCO^+ is actually tracing the interacting region.

Another HOCO^+ emission peak is located near the cloud M-0.02 - 0.07 (indicated by the central filled square in figure 2a), which is known as the +50 km s $^{-1}$ cloud. Both M-0.02 - 0.07 (the +50 km s $^{-1}$ cloud) and M-0.13 - 0.08 (the +20 km s $^{-1}$ cloud) are major gas condensations in the Sgr A region, having total masses of the order of $\sim 10^5 M_{\odot}$ (e. g., Güsten et al. 1981; Armstrong et al. 1985). M-0.02 - 0.07 also has been thought to be associated with the observed "molecular ridge" compressed by the expanding Sgr A East cloud, which lies just outside Sgr A East (Ho et al. 1985; Genzel et al. 1990; Serabyn et al. 1992). The elongated shape of the HOCO^+ emission in this region well resembles the distribution of the molecular ridge, but it does not agree with the general +50 km s $^{-1}$ cloud morphology. If the 50 km s $^{-1}$ cloud (M-0.02 - 0.07) is chemically quiescent and located far from the Galactic center compared to other condensations [as Minh et al. (2005) argued], this HOCO^+ elongation indicates that the abundance of this molecule also increases in the interacting region, like the +25 km s $^{-1}$ component of M-0.13 - 0.08. This cloud also coincides with the enhanced H_2 emission region, which is a region being shocked by interaction between the Sgr A East cloud and the ambient gas; it is likely to be associated with the +50 km s $^{-1}$ cloud (Lee et al. 2006).

The brightest HOCO^+ peak in the observed field was found at $(7', -5')$, which is close to the M0.11 - 0.08 (indicated by the leftmost filled square in figure 2a). This region has been considered to have a relatively smaller column density among the known condensations in this field (see Armstrong et al. 1985). Interestingly, the HCO^+ emission exhibits the strongest peak $2'$ south of the HOCO^+ peak near M0.07 - 0.08 (Minh et al. 2005). The large enhancement

of HCO^+ compared to ^{13}CO at this position strongly suggests that the formation of HCO^+ in this region does not proceed with CO , but with other shock related reactions involving the molecules such as C^+ or OH . Handa et al. (2006) showed a shell-like morphology of the $\text{SiO } J=1-0$ thermal emission in this region (which they assigned as G0.11 – 0.11). Their two peaks, A and B, which were not resolved in figures 2a and 2b due to the applied smoothing, coincide with our HOCO^+ and $^{29}\text{SiO } J=1-0$ peaks in position. Furthermore, their ridge (named E), which gives a strong peak in H^{13}CO^+ emission, was located $2'$ south of the HOCO^+ peak, where Handa et al. (2006) found the peak of the H_2 column density.

This region contains a lot of thermal and non-thermal features, indicating that shocks and high-energy photons play significant roles in characterizing this region (Figer et al. 2002; Yusef-Zadeh 2003). The 6.4 keV neutral Fe line was also detected in this region (Murakami et al. 2003). Thus the bright HOCO^+ emissions are all related with the regions which are thought to be affected by the strong Galactic center activities. This fact is a clue to understand the HOCO^+ emission in the Galactic-center molecular clouds. It also indicates that HOCO^+ may be a good tracer to probe the activities of the Galactic center.

Figure 2b shows the integrated intensity map of the $^{29}\text{SiO } J=1-0$ emission. It also exhibits triple peaks similar to HOCO^+ in figure 2a, which can be compared with the $\text{SiO } J=1-0$ emission map (Martin-Pintado et al. 1997). For the component associated with M 0.11 – 0.08, our $^{29}\text{SiO } J=1-0$ (and HOCO^+) distribution exhibits a good correlation with the $\text{SiO } J=1-0$ thermal emission (Handa et al. 2006) in general; figures 2a and 2b indicate stronger peaks at the positions A and B (though they were not resolved in our maps as mentioned), suggesting the $\text{SiO } J=1-0$ emission is optically thick [as found by Handa et al. (2006)].

It is well known that silicon, like the other heavy elements, is locked up in the refractory materials and shows a strong depletion in the gas phase in inactive dense clouds. The fractional abundance of the gas phase SiO relative to H_2 is observed to be less than 10^{-7} (Ziurys et al. 1989). Enhancement of SiO in the gas phase is thought to be related with shock waves, which are expected to erode and to partly destroy the dust through sputtering and grain-grain collisions (e.g., Pineau des Forets, & Flower 1997). The coincidence of the ^{29}SiO and the HOCO^+ emission regions again strongly suggests that the HOCO^+ enhancement is related with the shocks or Galactic center activities.

Figure 2c shows the $\text{H}53\alpha$ recombination line distribution. The emission peaks are located outside of the dense gas clouds. The strongest peak roughly coincides with HII region G0.10+0.02, observed by the 8.3 GHz continuum and $\text{H}92\alpha$ (Lang et al. 2001). It also coincides with the shocked diffuse cloud traced by the HCO^+ (Minh et al. 2005). In addition the well known arcs of the Galactic center are also located in this region. Therefore this recombination line traces diffuse shocked gas, which may result in the complicated ionized gas distribution.

4. Conclusion

We assigned the unidentified line U42.767 to the $2_{02}-1_{01}$ transition of HOCO^+ . The emission distribution in the Galactic center is quite similar to those found previously in the higher rotational transitions of this molecule. The past SiO maser surveys at ~ 43 GHz made at Nobeyama, which included the above transition in the same spectrometer, confirmed the rare existence of this ion except in Galactic center molecular clouds. It strongly suggests that CO_2 molecules are tightly frozen on dust grains in most of the Galactic clouds, but they are released from grains with other molecules such as SiO by shock activities in the Galactic center.

Authors thank Prof. William Irvine, University of Massachusetts, for reading the manuscripts, and Dr. Toshihiro Handa, University of Tokyo, and Dr. Shuro Takano, Nobeyama Radio Observatory, for helpful comments. They also thank the SiO maser survey team for allowing use of the data of the 2001–2003 and 2004–2005 SiO maser surveys. One of the authors (A. M.) thanks the National Astronomical Observatory for providing him with a visiting fellowship.

References

- Armstrong, J. T., Barrett, A. H., 1985, *ApJS*, 57, 535
Coil, A. L., & Ho, P. T. P., 2000. *ApJ*, 533, 245
Deguchi, S., Fujii, T., Miyoshi, M., & Nakashima, J. 2002, *PASJ*, 54, 61
Deguchi, S., et al. 2004, *PASJ*, 56, 261
Figer, D.F., et al. 2002. *ApJ* 581, 258
Fujii, T., Deguchi, S., Ita, Y., Izumiura, H., Kameya, O., Miyazaki, A., & Nakada, Y. 2006, *PASJ* 58, 529
Glass, I. S., Matsumoto, S., Carter, B. S., & Sekiguchi, K. 2001, *MNRAS*, 321, 77
Genzel, R., Stacey, G. J., Harris, A. I., Townes, C. H., Geis, N., Graf, U. U., Poglitsch, A., & Stutzki, J. 1990, *ApJ*, 356, 160.
Güsten, R., Walmsley, C.M., Pauls, T., 1981, *A&A* 103, 197.
Handa, T., Sakano, M., Naito, S., Hiramatsu, M., & Tsuboi, M. 2006, *ApJ*, 636, 261
Herbst, E., Green, S., Thaddeus, P., & Klemperer, W. 1977, *ApJ*, 215, 503
Ho, P. T. P., Jackson, J. M., Barrett, A. H., & Armstrong, J. T. 1985, *ApJ*, 288, 575.
Ho, P. T. P., Ho, L. C., Szczepanski, J. C., Jackson, J. M., Armstrong, J. T., & Barrett, A. H., 1991. *Nature* 350, 309.
Huettemeister, S., Dahmen, G., Mauersberger, R., Henkel, C., Wilson, T. L. & Martin-Pintado, J. 1998, *A&A*, 334, 646
Imai, H., et al. 2002, *PASJ*, 54, L19
Izumiura, H., Deguchi, S., Hashimoto, O., Nakada, Y., Onaka, T., Ono, T., Ukita, N., & Yamamura, I. 1995, *ApJ*, 453, 837
Kaifu, N. et al. 2004, *PASJ*, 56, 69

- Lang, C. C., Goss, W. M., & Morris, M. 2001, *AJ*, 121, 2681
- Lee, S. Pak, S., Choi, M., Davis, C. J., Geball, T. R. Herrnstein, R. M., Ho., P. T. P., Minh, Y. C., & Lee, S. 2006 (submitted to *ApJ*)
- Lilley, A. E. & Palmer, P. 1968, *ApJS*, 16, 143
- Lovas, 2004, *J. Phys. Chem. Ref. Data* 33, 177
- Martin-Pintado, J., de Vicente, P., Fuente, A. & Planesas, P. 1997, *ApJL*, 482, L45
- Minh, Y.C., Haikala, L., Hjalmarsen, Å., Irvine, W.M., 1998, *ApJ*, 498, 261.
- Minh, Y. C., Kim, S.-J., Pak, Soojong, Lee, Sungho, Irvine, W. M., Nyman, L. 2005, *New Astronomy*, 10, 425
- Minh, Y. C., Irvine, W. M., & Ziurys, L. M. 1988, *ApJ*, 334, 175
- Minh, Y. C., Brewer, M. K., Irvine, W. M., Friberg, P., & Johansson, L. E. B. 1991, *A&A*, 244, 470
- Miyazaki, A., Deguchi, S., Tsuboi, M., Kasuga, T., & Takano, S., 2001, *PASJ*, 53, 501
- Miyazaki, A., & Tsuboi, M., 2000, *ApJ*, 536, 357
- Murakami, H., Senda, A., Maeda, Y., & Koyama, K. 2003, *Astro. Nachr.*, 234, 125
- Oka, T., Hasegawa, T., Sato, F., Tsuboi, M., & Miyazaki, A. 1998, *ApJS*, 118, 455
- Okumura, S.K., et al. 1991, *ApJ* 378, 127
- Pickett, H. M. , Poynter, R. L. , Cohen, E. A. , Delitsky, M. L., Pearson, J. C., & Muller, H. S. P. 1998, *J. Quant. Spectrosc. & Rad. Transfer*, 60, 883
- Pineau des Forets, G. and Flower, D. 1997, *IAU Symp. 178, Molecules in Astrophysics*, ed. E. F. van Dishoeck, 113.
- Serabyn, E., Lacy, J. H., & Achterman, J. M., 1992. *ApJ*, 395, 166.
- Shiki, S., Ohishi, M. & Deguchi, S. 1997, *ApJ*, 478, 206
- Thaddeus, P., Guelin, M., & Linke, R. A. 1981, *ApJL*, 246, L41
- Tsuboi, M. Handa, T., & Ukita, N., 1999, *ApJS*, 120, 1
- Turner, B.E., Terzieva, R., & Herbst, E. 1999, *ApJ*, 518, 699.
- van Dishoeck, E. F. 2004, *ARA&A*, 42, 119
- Yusef-Zadeh, F. 2003, *ApJ*, 598, 325.
- Ziurys, L. M., Friberg, P., & Irvine, W. M. 1989, *ApJ*, 343, 201

Table 1. Rest frequencies adopted.

species	transition	frequency (MHz)	reference
HOCO ⁺	$J_{K_a, K_b} = 2_{02}-1_{01}$	42766.198	Pickett et al. 1998
SiO	$J = 1-0 \ v = 2$	42820.582	Lovas et al. 2004
²⁹ SiO	$J = 1-0 \ v = 0$	42879.922	Lovas et al. 2004
H	53 α	42951.97	Lilley & Palmer 1968
He	53 α	42969.48	Lilley & Palmer 1968

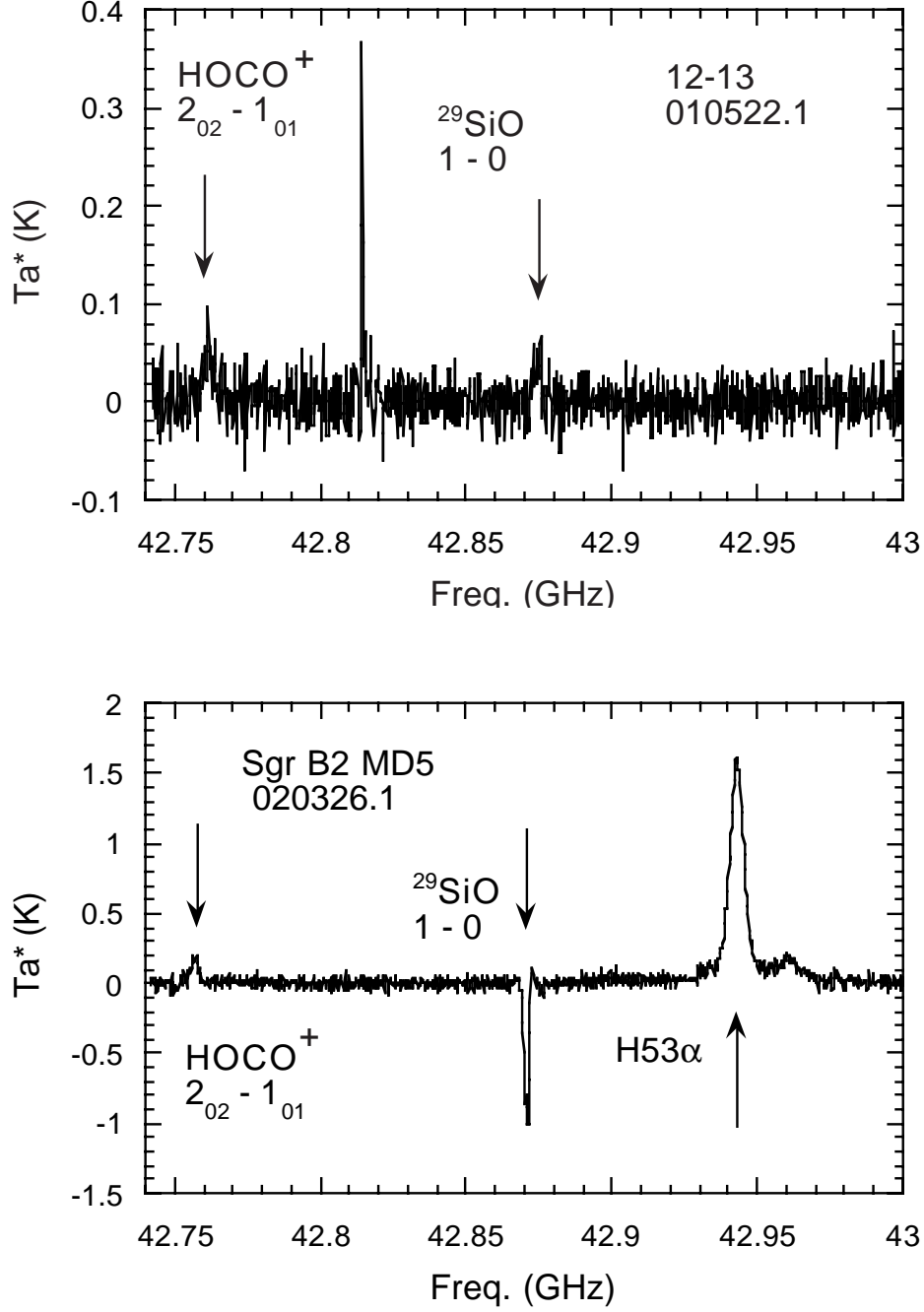


Fig. 1. AOS-W Spectra between 42.74 and 43.0 GHz toward [GMC2001] 12-13 (upper panel) and toward Sgr B2 MD5 (lower panel). The observational date was shown in yymmdd.d format under the object name. The sharp strong line at 42.82 GHz in the upper panel is the $\text{SiO } J=1-0 \ v=2$ maser line from [GMC2001] 12-13. On the right of $\text{H53}\alpha$, a weak enhancement due to $\text{He53}\alpha$ is recognizable in the lower panel.

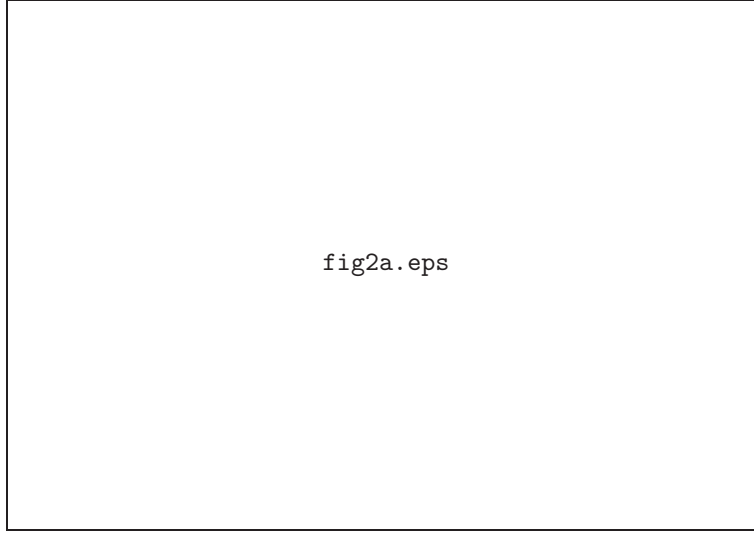


Fig. 2. a. Integrated intensity map of the $\text{HOCO}^+ 2_{02}-1_{01}$ emission toward the Galactic center. The observed positions are marked by crosses. The contours are drawn by every 0.3 K km s^{-1} to the peak flux of 4 K km s^{-1} . The outer lines near corners indicate the outer boundary of the sampled positions. The filled squares indicate the positions of M0.11–0.08, M–0.02 – 0.07, and M–0.13 – 0.08, from the left to the right.



Fig. 2. b. Integrated intensity map of the $^{29}\text{SiO } J = 1-0 \ v = 0$ emission toward the Galactic center. The observed positions are marked by crosses. The contours are drawn by every 0.3 K km s^{-1} to the peak flux of 2.8 K km s^{-1} . The filled squares indicate the positions of M0.11–0.08, M–0.02 – 0.07, and M–0.13 – 0.08, from the left to the right.



Fig. 2. c. Integrated intensity map of H53 α toward the Galactic center. The observed positions are marked by crosses. The contours are drawn by every 0.3 K km s⁻¹ to the peak flux of 3.5 K km s⁻¹. The filled squares indicate the positions of M0.11–0.08, M–0.02 – 0.07, and M–0.13 – 0.08, from the left to the right.

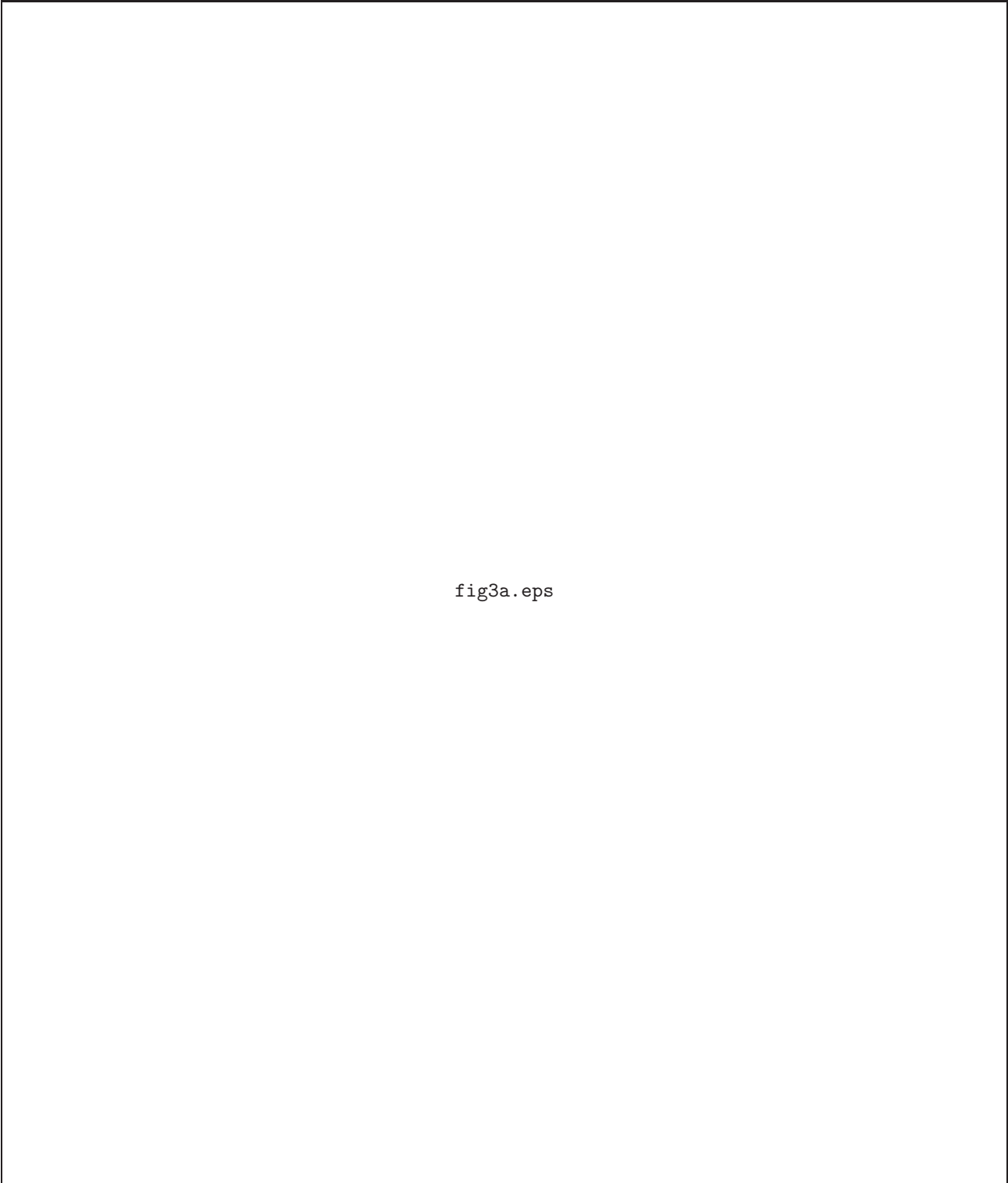
The figure is a velocity-channel map showing the intensity of the HOCO+ $JKK = 2_{02}-1_{01}$ emission. The map is presented as a grayscale image with overlaid contours. The contours represent intensity levels, starting from a baseline and increasing to a peak temperature of 0.101 K. The map is centered on the Galactic center. The text "fig3a.eps" is centered within the plot area.

fig3a.eps

Fig. 3. a. Velocity-channel map of the HOCO^+ $JKK = 2_{02}-1_{01}$ emission toward the Galactic center. The contours are drawn by every 0.01 K to the peak temperature of 0.101 K.

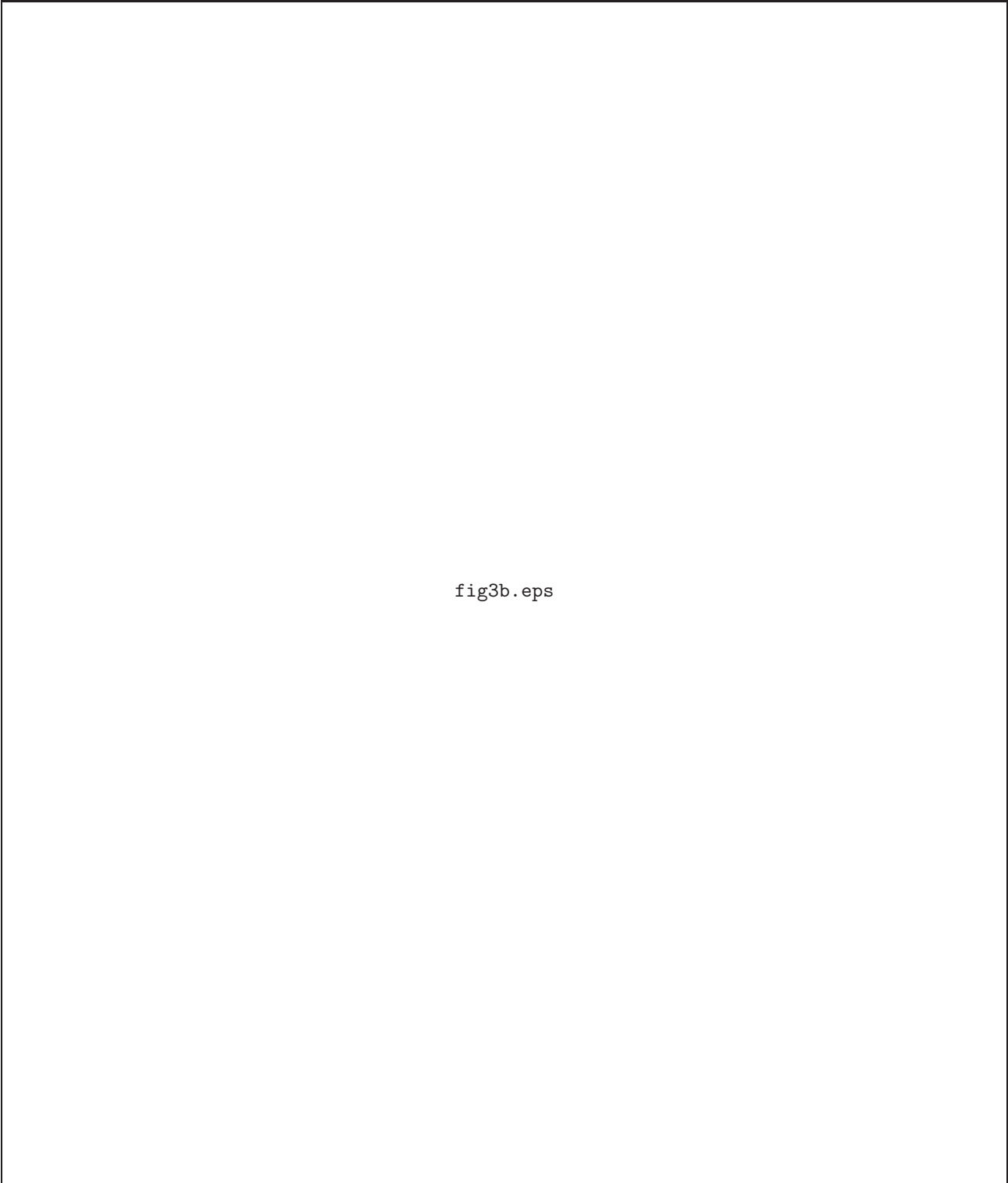
The figure is a velocity-channel map, which typically consists of a 2D spatial map with a color bar on the right indicating intensity or temperature. The map shows the distribution of the ^{29}SiO $J=1-0$ $v=0$ emission. The color bar would range from 0 to 0.084 K, with contours drawn every 0.01 K. The spatial distribution would show the emission source and its extent in the sky.

fig3b.eps

Fig. 3. b. Velocity-channel map of the ^{29}SiO $J = 1-0$ $v = 0$ emission toward the Galactic center. The contours are drawn by every 0.01 K to the peak temperature of 0.084 K.

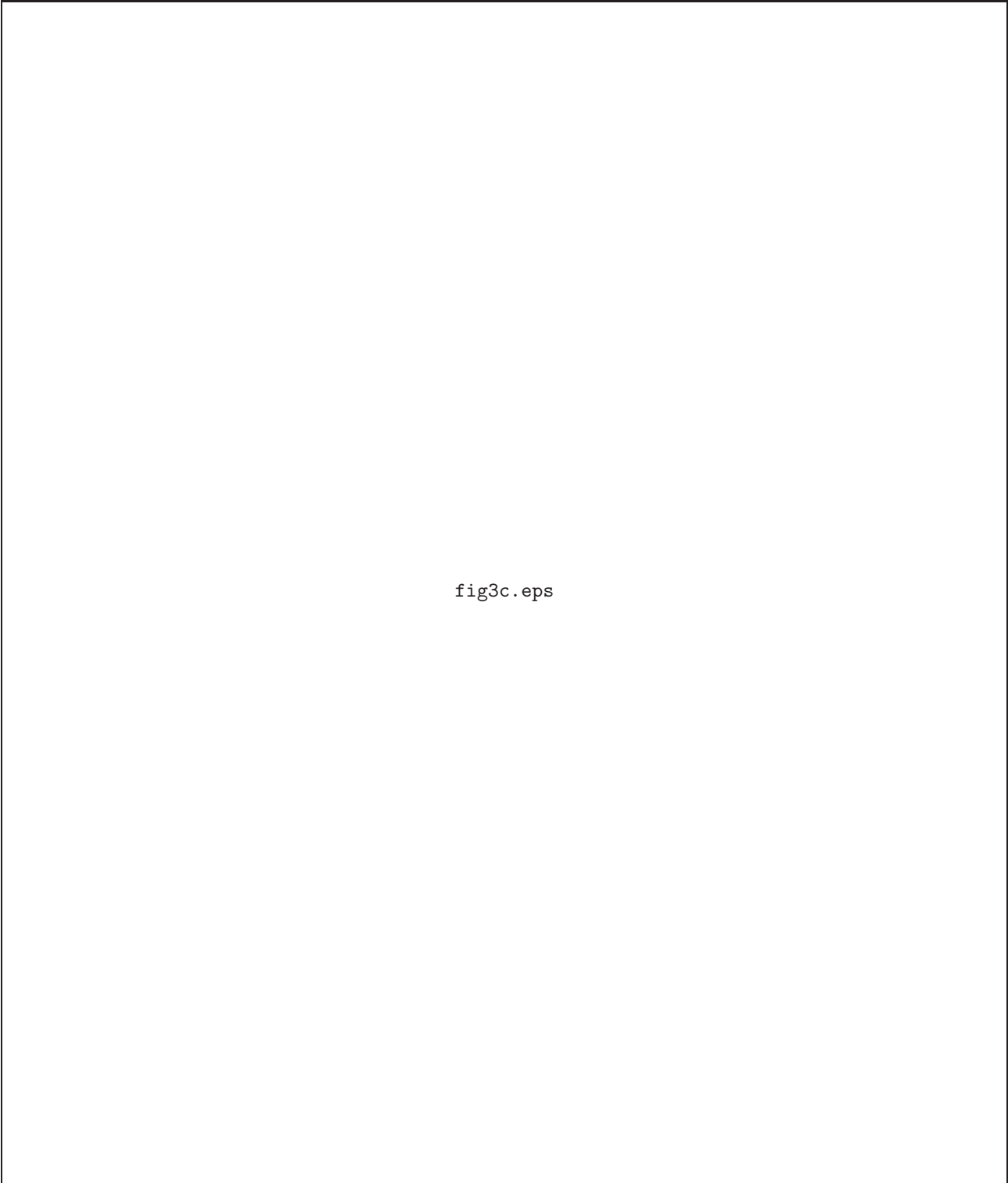
The figure is a velocity-channel map of H53α emission toward the Galactic center. It is a square plot with a grayscale color bar on the right side. The color bar ranges from 0.00 to 0.081 K, with major ticks every 0.01 K. The map shows a complex pattern of emission, with a prominent bright region in the upper left quadrant and a more diffuse, elongated structure extending from the center towards the lower right. The text 'fig3c.eps' is centered within the plot area.

fig3c.eps

Fig. 3. c. Velocity-channel map of H53 α toward the Galactic center. The coutours are drawn by every 0.01 K to the peak temperature of 0.081 K.

This figure "fig2a.jpg" is available in "jpg" format from:

<http://arXiv.org/ps/astro-ph/0609625>

This figure "fig2b.jpg" is available in "jpg" format from:

<http://arXiv.org/ps/astro-ph/0609625>

This figure "fig2c.jpg" is available in "jpg" format from:

<http://arXiv.org/ps/astro-ph/0609625>

This figure "fig3a.jpg" is available in "jpg" format from:

<http://arXiv.org/ps/astro-ph/0609625>

This figure "fig3b.jpg" is available in "jpg" format from:

<http://arXiv.org/ps/astro-ph/0609625>

This figure "fig3c.jpg" is available in "jpg" format from:

<http://arXiv.org/ps/astro-ph/0609625>